ENGINEERING TRANSACTIONS • *Engng. Trans.* • 40, 1, 103-113, 1992
Polish Academy of Sciences • Institute of Fundamental Technological Research

LARGE DISPLACEMENTS IN TIRE INFLATION PROBLEM

J. P E L C (OLSZTYN)

In the paper a method for pneumatic tire structural analysis is described, taking into account large displacements and cord-rubber plies material properties. Axisymmetrical state of deformation is considered. The developed numerical algorithms and computer codes are verified by solving some benchmark problems. Simplified radial truck tire model is used for this purpose. The results were found to be in good agreement with other available data.

1. INTRODUCTION

Pneumatic tire is a structure which consists of various rubber compounds and cord-rubber plies, i.e. rubber layers with cord reinforcement (Fig.1). Complex geometry, large displacemens and strains under service loading, nonlinear material characteristics and complicated loading conditions are a source of serious problems in pneumatic tire structural analyses. Nevertheless, reasonable designing process makes the analyses to be carried out before the tire has been manufactured. Numerical simulation of real tire response during operation loading has even appeared to be less time-consuming as well as less expensive than experiments.

There have been written many papers on pneumatic tire modeling and computations. Quite a number of references one can find in papers [1, 2, 3]. In recent years the main efforts were concentrated upon finite element tire model development and improvement [2, 4].

In the paper a method is described which incorporates the orthotropic material properties of cord-rubber composite to the structural analysis of a tire. Large displacements are taken into account in the analysis. Numerical procedures have been worked out and then implemented into the

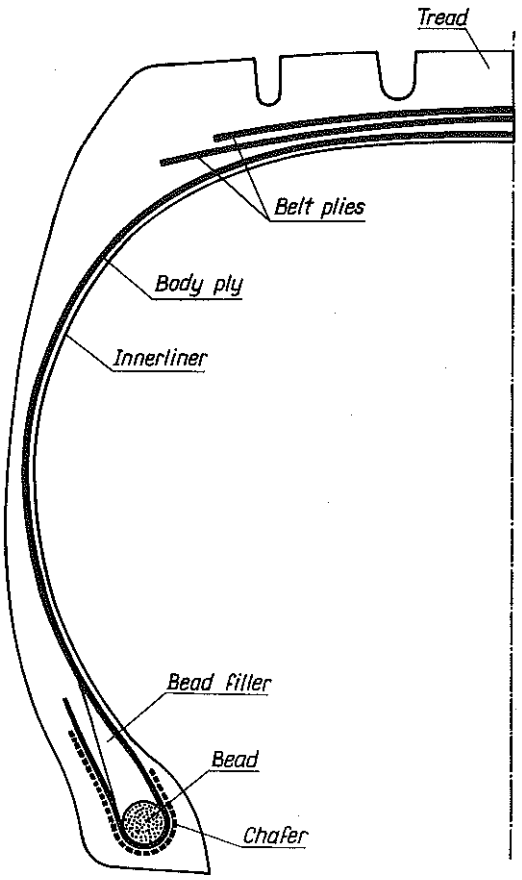

FIG. 1. Pneumatic tire cross-section.

finite element program[1] to tackle the pneumatic tire inflation problem. The structure undergoes large displacements, Total Lagrangian (T.L.) formulation presented by BATHE [5] being used to derive nonlinear equilibrium equations for the structure. Material was assumed to be linear elastic, homogeneous and orthotropic. Permissibility of such assumptions was discussed and justified in [6]. Cord-rubber elastic constants were obtained from the Halpin-Tsai equations [7]. Nonlinear equations of the finite element method have been solved using Newton-Raphson technique. The procedure described by CRISFIELD [8] was employed to control the solution process. Isoparametric axisymmetrical finite elements have been used in the analy-

[1]The program has been developed at the Institute of Structural Mechanics, Warsaw University of Technology.

sis. The algorithms and the computer code have been verified on two test problems. The results are in good agreement with those obtained otherwise.

2. Incremental equations of deformable body motion

Deformation process of a body may be described by Green-Lagrange strain tensor ${}^t_0E_{ij}$. From here on superscript t and subscript 0 indicate the object to be considered at time t with respect to time $t = 0$, i.e. the object is referred to the initial configuration of a body. The main feature of the strain tensor being utilized here is its insensitivity to rigid body motion. This type of motion occurs in elements of cord-rubber structure. Furthermore, the 2nd Piola-Kirchhoff stress tensor appears to be energetically conjugate to the Green-Lagrange strain tensor, and both are used in T.L. formulation of nonlinear problems. The virtual work principle may be written as

$$\int_{{}^0V} {}^{t+\Delta t}_0S_{ij}\,\delta\,{}^{t+\Delta t}_0E_{ij}\,{}^0dV = {}^{t+\Delta t}W\,, \tag{2.1}$$

where ${}^0V$ – volume of a body at time $t = 0$, ${}^{t+\Delta t}W$ – virtual work done by the externally applied forces on the corresponding virtual displacements at time $t + \Delta t$.

Performing the decomposition

$$\begin{aligned} {}^{t+\Delta t}_0S_{ij} &= {}^t_0S_{ij} + {}_0S_{ij}\,, \\ {}^{t+\Delta t}_0E_{ij} &= {}^t_0E_{ij} + {}_0E_{ij}\,, \\ {}_0E_{ij} &= {}_0e_{ij} + {}_0\eta_{ij}\,, \end{aligned} \tag{2.2}$$

where ${}_0e_{ij}$ and ${}_0\eta_{ij}$ are the linear and nonlinear parts of strain tensor increment with respect to displacements increment, respectively, and assuming that

$$\begin{aligned} {}_0S_{ij} &= {}_0D_{ijkl}\,{}_0e_{kl}\,, \\ \delta\,{}_0E_{ij} &= \delta\,{}_0e_{ij}\,, \end{aligned} \tag{2.3}$$

the principle of virtual work may be rewritten in the following form:

$$\int_{{}^0V} {}_0D_{ijkl}\,{}_0e_{kl}\,\delta\,{}_0e_{ij}\,{}^0dV + \int_{{}^0V} {}^t_0S_{ij}\,\delta\,{}_0\eta_{ij}\,{}^0dV = {}^{t+\Delta t}W - \int_{{}^0V} {}^t_0S_{ij}\,\delta\,{}_0e_{ij}\,{}^0dV\,. \tag{2.4}$$

On the basis of Eq. (2.4) one can determine a displacements vector increment and then, using Eq. (2.2), current strains and stresses are computed. However, Eq. (2.1) is no longer satisfied with the obtained displacements because of the approximation (2.3). So the right-hand side of Eq. (2.4) is replaced by unbalanced virtual work, and the subsequent displacements vector increment may be obtained. In this way an iterative process has been involved in the incremental procedure.

3. Finite element method equilibrium equation

With the coordinates and displacements being approximated within the element, formula (2.4) yields the following equilibrium equation in the matrix form:

$$\left({}_0^t\mathbf{K}_L + {}_0^t\mathbf{K}_{NL}\right)\Delta\mathbf{u}^{(i)} = {}^{t+\Delta t}\mathbf{R} - {}_0^{t+\Delta t}\mathbf{F}^{(i-1)}, \tag{3.1}$$

where

$$\Delta\mathbf{u}^{(i)} = {}^{t+\Delta t}\mathbf{u}^{(i)} - {}^{t+\Delta t}\mathbf{u}^{(i-1)},$$
$${}^{t+\Delta t}\mathbf{u}^{(0)} = {}^{t}\mathbf{u}, \qquad {}_0^{t+\Delta t}\mathbf{F}^{(0)} = {}_0^t\mathbf{F}.$$

Superscripts in brackets denote the number of iteration.

$${}_0^t\mathbf{K}_L = \int_{{}^0V} {}_0^t\mathbf{B}_L^T \, {}_0\mathbf{D} \, {}_0^t\mathbf{B}_L \, {}^0dV,$$

$${}_0^t\mathbf{K}_{NL} = \int_{{}^0V} {}_0^t\mathbf{B}_{NL}^T \, {}_0^t\mathbf{S} \, {}_0^t\mathbf{B}_{NL} \, {}^0dV,$$

$${}_0^t\mathbf{F} = \int_{{}^0V} {}_0^t\mathbf{B}_L^T \, {}_0^t\hat{\mathbf{S}} \, {}^0dV.$$

${}^{t+\Delta t}\mathbf{R}$ – externally applied nodal forces vector at time $t + \Delta t$.

Strain-displacement transformation matrix ${}_0^t\mathbf{B}_L$ is a sum of two matrices: ${}_0^t\mathbf{B}_{L0}$ – with elements being only functions of elements interpolation functions, ${}_0^t\mathbf{B}_{L1}$ – with elements being functions of displacements ${}^t\mathbf{u}$. The latter matrix may be expressed in a convenient form:

$${}_0^t\mathbf{B}_{L1} = {}_0^t\mathbf{A}_Q \, {}_0^t\mathbf{B}_{NL}, \tag{3.2}$$

where ${}_0^t\mathbf{B}_{NL}$ again consists of the same elements as matrix ${}_0^t\mathbf{B}_{L0}$. Matrix ${}_0^t\mathbf{A}_Q$ is constructed from elements of the vector

$${}_0^t\mathbf{Q} = {}_0^t\mathbf{B}_{NL} \, {}^t\mathbf{u}. \tag{3.3}$$

Furthermore: ${}_0\mathbf{D}$ – material property matrix, ${}^t_0\mathbf{S}$, ${}^t_0\hat{\mathbf{S}}$ – 2nd Piola - Kirchhoff stresses matrix and vector, respectively.

It should be noted that all derivatives that enter ${}^t_0\mathbf{B}_L$ and ${}^t_0\mathbf{B}_{NL}$ are referred to the initial configuration of a body. Matrices ${}^t_0\mathbf{B}_{L0}$ and ${}^t_0\mathbf{B}_{NL}$ remain constant during incremental/iterative process of solving nonlinear equilibrium equations.

Since linear elastic material was assumed, the matrix $\mathbf{D}$ is constant in the constitutive relation

$$ {}^t_0\mathbf{S} = \mathbf{D}\, {}^t_0\mathbf{E} \,. \tag{3.4}$$

Green - Lagrange strains vector is a nonlinear function of the nodal displacements

$$ {}^t_0\mathbf{E} = ({}^t_0\mathbf{B}_{L0} + 0.5\, {}^t_0\mathbf{B}_{L1})\, {}^t\mathbf{u} \,, \tag{3.5}$$

whereas linear part of its increment ${}_0\mathbf{e}$ is a linear function of the nodal displacements increment $\Delta\mathbf{u}$:

$$ {}_0\mathbf{e} = ({}^t_0\mathbf{B}_{L0} + {}^t_0\mathbf{B}_{L1})\Delta\mathbf{u} \,. \tag{3.6}$$

4. Cord-rubber material elasticity matrix

Cord-rubber plies are the basic structural components of the pneumatic tire. The aim of the following considerations is to determine the elasticity matrix for rubber layer reinforced with cords. The matrix should be expressed in the coordinate system (x, y, ϕ) in which computations are to be carried out. We have chosen the y-axis to be the symmetry axis of the tire. Effective elastic constants for a ply (Fig.2) are evaluated on the basis of Halpin - Tsai equations [7]:

$$\begin{aligned} E_1 &= E_c v_c + E_r(1 - v_c) \,, \\ E_2 &= E_r(1 + 2v_c)/(1 - v_c) \,, \\ G_{12} &= G_r(1 + \kappa)/(1 - \kappa) \,, \\ \nu_{12} &= \nu_c v_c + \nu_r(1 - v_c) \,, \\ \nu_{21} &= \nu_{12} E_2 / E_1 \,, \end{aligned} \tag{4.1}$$

where

$$ \kappa = v_c(G_c - G_r)/(G_c + G_r) \,, $$

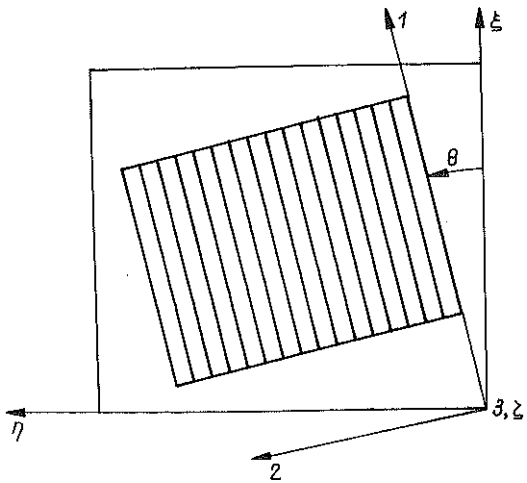

FIG. 2. Principal axes (1,2,3) for cord-rubber layer.

E_c, E_r – Young's moduli of cord/rubber, G_c, G_r – shear moduli of cord/rubber, ν_c, ν_r – Poisson's ratios of cord/rubber, v_c – volume fraction of the cord in a ply.

These relations allow to assess the following parameters for the one-ply cord-rubber system: longitudinal Young's modulus E_1, the transverse Young's modulus E_2, the in-plane shear modulus G_{12}, the major Poisson's ratio ν_{12}, and the secondary Poisson's ratio ν_{21}. Superscripts 1 and 2 indicate the axes parallel and perpendicular to the cord direction, respectively. The major Poisson's ratio ν_{12} is associated with a contraction in the 2 direction caused by a uniaxial tensile stress in the direction 1. Due to the reciprocity relation $(4.1)_5$ there are only four independent elastic constants for an orthotropic ply. These so-called average or smeared constants characterize the macroscopic property of a cord-rubber composite. They were derived on the basis of micromechanics approach to a material model, use being made of the properties of cord and rubber and their concentration. In addition, the assumptions were made: cord cross-section was nominally circular and E_c was much greater than E_r.

Assuming that the material is transversely isotropic in the 2-3 plane, we have

$$E_3 = E_2\,, \qquad \nu_{13} = \nu_{12}\,, \qquad G_{13} = G_{12}\,. \tag{4.2}$$

Following CEMBROLA and DUDEK [9] we have taken $G_{23} = 2G_{12}$. Thus

matrix ${}^t_0\mathbf{D}^1$ in the constitutive equation

$$ {}^t_0\mathbf{S}^1 = {}^t_0\mathbf{D}^1 \, {}^t_0\mathbf{E}^1 \tag{4.3} $$

was determined. The stresses and strains are arranged in vectors

$$ \begin{aligned} {}^t_0\mathbf{S}^1 &= \left[{}^t_0S^1_{11},\ {}^t_0S^1_{22},\ {}^t_0S^1_{12},\ {}^t_0S^1_{33},\ {}^t_0S^1_{13},\ {}^t_0S^1_{23}\right]^T , \\ {}^t_0\mathbf{E}^1 &= \left[{}^t_0E^1_{11},\ {}^t_0E^1_{22},\ 2{}^t_0E^1_{12},\ {}^t_0E^1_{33},\ 2{}^t_0E^1_{13},\ 2{}^t_0E^1_{23}\right]^T . \end{aligned} \tag{4.4} $$

The superscript on the right-hand side of a symbol indicates the first axis of right-handed coordinate system in which the symbol is defined.

To express Eq. (4.3) in the $(\xi\eta\zeta)$ coordinate system, the transformations are necessary:

$$ {}^t_0\mathbf{S}^1 = \mathbf{T}_\theta \, {}^t_0\mathbf{S}^\xi , \qquad {}^t_0\mathbf{E}^1 = \tilde{\mathbf{T}}_\theta \, {}^t_0\mathbf{E}^\xi , \tag{4.5} $$

where

$$ \mathbf{T}_\theta = \begin{bmatrix} c^2 & s^2 & 2sc & & & \\ s^2 & c^2 & -2sc & & & \\ -sc & sc & c^2 - s^2 & & & \\ & & & 1 & & \\ & & & & c & s \\ & & & & -s & c \end{bmatrix} , $$

$c = \cos\theta$, $s = \sin\theta$, and $\tilde{T}_\theta$ is obtained from T_θ by multiplying its 3rd column by 0.5. Substitution of Eq. (4.5) into Eq. (4.3) leads to

$$ {}^t_0\mathbf{S}^\xi = (\mathbf{T}_\theta^{-1} \, {}^t_0\mathbf{D}^1 \tilde{\mathbf{T}}_\theta) \, {}^t_0\mathbf{E}^\xi = {}^t_0\mathbf{D}^\xi \, {}^t_0\mathbf{E}^\xi . \tag{4.6} $$

One more transformation is required as the normal to a ply changes its direction along the ply in the $(x,\ y,\ \phi)$ system (Fig.3). Appropriate column and row arrangement of the ${}^t_0\mathbf{D}^\xi$ matrix makes the transformation matrix $\mathbf{T}_\alpha$ identical with the $\mathbf{T}_\theta$ matrix, but with $c = \cos\alpha$ and $s = \sin\alpha$. Finally we obtain:

$$ {}^t_0\mathbf{D}^x = \mathbf{T}_\alpha^{-1} \, {}^t_0\mathbf{D}^\zeta \, \tilde{\mathbf{T}}_\alpha . \tag{4.7} $$

When axisymmetrical problem is considered ${}^t_0E_{\xi\eta} = {}^t_0E_{\xi\zeta} = 0$, and element strain and stress vector are four-element vectors. Then the corresponding elastic matrices are 4 by 4 matrices.

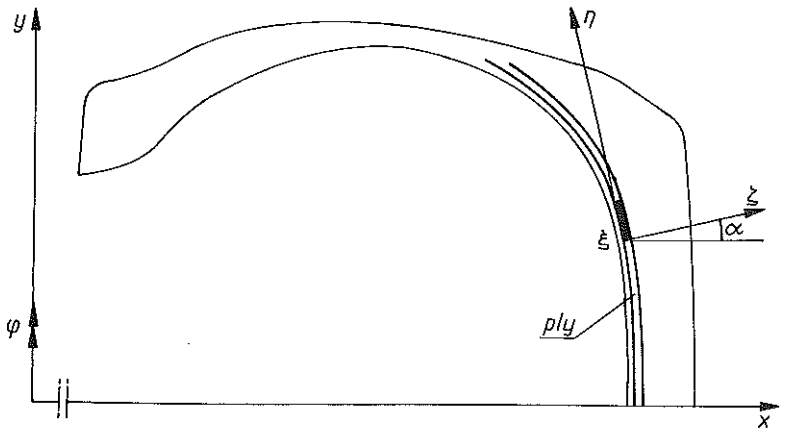

FIG. 3. Finite element location within tire profile defined by local coordinate system (ξ, η, ζ).

5. NUMERICAL EXAMPLES

To test the procedures described in previous paragraphs, two numerical examples were made by means of the finite element method program in which the procedures had been implemented.

The first task is the well-known problem of thin isotropic shallow spherical cap under apex load. Numerical data have been taken from paper [10] by BATHE, RAMM and WILSON. The structure is highly nonlinear as the snap-through phenomenon occurs when the load is increasing. Ten 8-node elements were used to the analysis. The load-deflection curve obtained for the shell was found to be identical with that presented in [10].

The second test pertains to the radial 11.00R20 truck tire inflation analysis (internal pressure loading only). A simplified tire model composed of a body ply ($\theta = 90°$) and two belt plies ($\theta = 20°$, $\theta = -20°$) was considered (Fig. 4). Only one half of cross-section of the tire was modeled due to symmetry. X-axis was assumed to be the axis of symmetry. Initial profile of a tire was determined using the netting analysis [11]. Thickness of each ply was taken to be equal to 2.8 mm. Two belt plies were grouped into a band. Finite element discretization of body ply and the band was such that each finite element represented one ply or one band thickness. For the material of the band, terms of the elasticity matrix associated with $\xi\eta\zeta$ coordinate system were computed as weighted average values of the corresponding terms entered ${}^{t}_{0}\mathbf{D}^{\xi}$ matrices formulated for each belt ply separately. Finite element

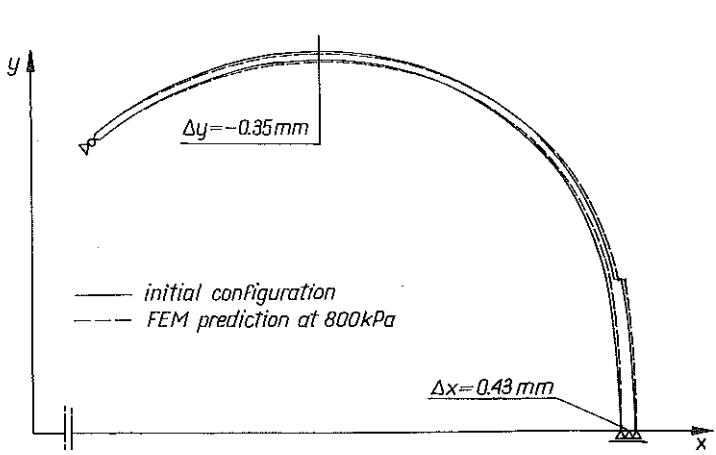

FIG. 4. Simplified radial truck tire model.

discretization was: six 8-node elements within the belt plies domain; thirty two 8-node elements and a 6-node element within the body ply. A total of 39 elements (186 nodes, 365 degrees of freedom) were used in the finite element simplified tire model. Under Crisfield's control procedure, only seven load steps have been used up to a full inflation pressure of 800 kPa. All load steps were iterated to reach a converged solution. Small displacements were obtained in the finite element analysis as the initial configuration really was the equilibrium configuration of the tire. The mid-surface point at the crown moved outside by $\Delta x = 0.43$ mm and the point at the sidewall moved inside the tire by 0.35 mm.

More rigorous test takes place when one is inflating the tire after having rejected the belt plies. Then the initial configuration of the structure is far from the equilibrium configuration and the structure possesses practically no stiffness. 33 elements (166 nodes, 327 degrees of freedom) were used in this case. Iterative process convergence rate was extremely slow and up to the 106 load steps (with the same iteration process parameters as in the previous task) were necessary to reach about 100 kPa internal pressure. Body ply profile at about 100 kPa is shown in Fig.5. The magnitude of the internal pressure indicates the moment at which the structure begins to stiffen. Further pressure growth would lead to cord's length increase. The growth in the radius of the body ply is 23.4 mm and the decrease of the half cross-section width is 10.6 mm. Differences between the net model prediction and the present analysis results have appeared to be small: $\delta x = 0.15$ mm at the crown and 0.43 mm at the maximum width point. Thus

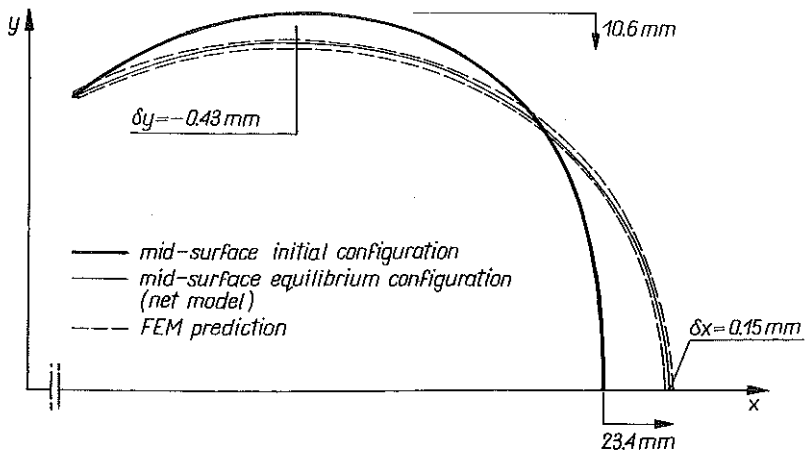

FIG. 5. Equilibrium configuration of unbelted tire.

the results are in good agreement with that known from the netting analysis which assumes the cord to be inextensible.

6. FINAL REMARKS

Pneumatic tire structural analysis requires large displacements to be taken into account as they may occur when the initial configuration of a designed tire is far from the equilibrium configuration or under service loading of a tire. Finite element method seems to be the unique analytical tool for the tire analysis. It makes it possible to investigate many important effects. For instance: interply shear strains, bending effects in truck tires and so on. These effects are neglected in the netting analysis – the most frequently method used in the tire design process.

On the basis of the numerical tests we can regard the program to run correctly and accurately. We hope it to be useful in scheming a new tire constructions and in improving the present ones. The program is being developed to include such effects as nonlinear material characteristics, nonconservative loading etc.

REFERENCES

1. R.A.RIDHA, *Computation of stresses, strains and deformations of tires*, Rubb. Chem. Technol., **53**, 4, pp. 849-902, 1980.

2. A.K.NOOR and J.A.TANNER, *Tire modeling and contact problems: advances and trends in the development of computational models for tires*, Comput. Struct., **20**, 1-3, pp. 517-533, 1985.

3. J.PELC, *Pneumatic tire computational models a survey*, [in Polish], Theor. Appl. Mech., **29**, 3-4, pp. 709-725, 1991.

4. F.TABADDOR and J.R.STAFFORD, *Some aspects of rubber composite finite element analysis*, Comput. Struct., **21**, 1/2, pp. 327-339, 1985.

5. K.J. BATHE, *Finite element procedures in engineering analysis*, Prentice-Hall, Englewood Cliffs, New York 1982.

6. H.P.PATEL, J.L.TURNER and J.D.WALTER, *Radial tire cord-rubber composites*, Rubb. Chem. Technol., **49**, 4, pp. 1095-1110, 1976.

7. J.D.WALTER, *Cord-rubber tire composites: theory and applications*, Rubb. Chem. Technol., **51**, 3, pp. 524-576, 1978.

8. M.A.CRISFIELD, *A fast incremental/iterative solution procedure that handles "snap-through"*, Comput. Struct., **13**, pp. 55-62, 1981.

9. R.J.CEMBROLA and T.J.DUDEK, *Cord/rubber material properties*, Rubb. Chem. Technol., **58**, 4, pp. 830-856, 1985.

10. K.J.BATHE, E.RAMM and E.L.WILSON, *Finite element formulations for large deformation dynamic analysis*, Int. J. Num. Meth. Eng., **9**, 9, pp. 353-386, 1975.

11. J.PELC and E.PETZ, *Computer aid in inner tire profile design*, [in Polish], Polimery, **33**, 10, pp. 381-383, 1988.

DEPARTMENT OF MECHANICAL ENGINEERING
AGRICULTURAL AND TECHNICAL ACADEMY, OLSZTYN.

Received April 24, 1991.